Available online at www.sciencedirect.com
ScienceDirect
Carbohydrate Polymers 68 (2007) 122–127
Carbohydrate Polymers
www.elsevier.com/locate/carbpol

Effect of *N*-acylation on structure and properties of chitosan fibers

Choong Youl Choi [a], Su Bong Kim [a], Pyong Ki Pak [a], Dong Il Yoo [b], Yong Sik Chung [a,*]

[a] *Department of Textile Engineering, Chonbuk National University, Joenju, 561-756, Republic of Korea*
[b] *Department of Textile Engineering, Chonnam National University, Gwangju, 500-757, Republic of Korea*

Received 17 May 2006; received in revised form 14 July 2006; accepted 18 July 2006
Available online 1 September 2006

Abstract

This article described the physico-chemical transition of the chitosan fibers by *N*-acylation. *N*-Acyl chitosan fibers were prepared by a post-treatment of chitosan fibers with carboxylic anhydrides (e. q., acetic, propionic, butyric, hexanoic anhydride) in methanol at room temperature. *N*-Acyl chitosan fibers were analyzed by FT-IR, TGA, DSC, XRD and SEM. *N*-Acylation with longer hydrocarbon side chain resulted in a higher spatial organization of the chain to the long axis and showed lower moisture retention. The *N*-acyl chitosan fibers with short acyl chain exhibited gradually lower tensile strength. *N*-Hexanoyl chitosan fibers showed higher tensile strength than *N*-acetylated ones. The chemical structure of chitosan fibers was gradually altered from hydrated form (anti-parallel structure) to dehydrated form (parallel structure) with a treatment of carboxylic anhydrides.

Keywords: Chitosan fibers; *N*-Acylation; *N*-Acylchitosan fibers; Carboxylic anhydrides; Chemical structure transition

1. Introduction

Chitin[Poly-(1 → 4)-2-acetamido-2-deoxy-β-D-glucose] and chitosan[Poly-(1 → 4)-2-amino-2-deoxy-β-D-glucose] are natural polymers extracted from various plants and animals. In recent years, these two polymers have attracted much interest because of their non-toxicity, biodegradability, biocompatibility, wound-healing acceleration and many other unique properties (Majuti & Kumar, 2000; Mori et al., 1997; Shigemasa & Minami, 1995). As a natural renewable resource, they offer many potential applications in a number of diversified fields such as biomedical materials, biodegradable packaging, cosmetics, heavy metal ion absorbent and textile goods.

In particular, their use in the textile industry, with a much larger scope, could be a long-term possibility (George & Yimin, 1993). However, the application of chitosan fibers in the above area is still limited. The main reason for this limitation is the level of difficulty involved in handling during the processing because the chitosan fibers are too weak even in the diluted acidic solvent and common chemicals. This drawback of chitosan fibers enhances chemical reactivity in comparison with chitin.

Consequently, many studies have dealt with the chemical modification to introduce hydrophobic nature to chitosan such as phthaloylation, alkylation and acylation reaction (Hirano, Ohe, & Ono, 1976; Hirano & Noishiki, 1985; Hirano & Midorikawa, 1998; Hirano, Zhang, Chung, & Kim, 2000). Since chitosan has two hydroxyl groups and one amino group per glucoseamine unit, several new chitosan derivatives have been produced with the modification of these groups, and the resulting polymer shows a unique original chitosan molecule. Strong intra-molecular and intermolecular hydrogen bonds exist in chitosan to form random orientations. The dissociation and reorganization of these hydrogen bonds by chemical modification facilitates the production of novel molecular conformations in the forms of solutions, hydrogels, fibers, films and sponges (Tokura et al., 1990).

The complete crystalline structure of chitosan has been described (Kawada, Abe, Yui, Okuyama, & Ogawa, 1999; Mohamed, Subban, & Arof, 1995; Samuels, 1981; Yui et al., 1994). Generally, three forms, hydrated, dehydrated and

* Corresponding author. Tel.: +82 63 270 2350; fax: +82 63 270 2348.
E-mail address: psdcolor@chonbuk.ac.kr (Y.S. Chung).

0144-8617/$ - see front matter © 2006 Elsevier Ltd. All rights reserved.
doi:10.1016/j.carbpol.2006.07.018

noncrystalline structures, of solid chitosan are found (Clark & Smith, 1937; Okuyama, Noguchi, Miyazawa, Yui, & Ogawa, 1997; Rudall, 1963). The crystalline structure of hydrated chitosan is a twofold helix, which can be converted to a dehydrated form by dehydration or annealing, very similar to the hydrated form, but with the molecular packing and water content quite different (Okuyame et al., 2000).

The object of our study was to observe the transition in the chemical structure and physico-chemical properties of chitosan fibers by introducing the hydro-carbon side chain using various carboxylic anhydrides. We prepared *N*-acylchitosan fibers with a series of carboxylic anhydrides, which was proposed by Hirano et al., and characterized by elemental analysis, and Fourier-transform infrared analysis. Also, the structure and physico-chemical properties of these derived chitosan fibers were examined by X-ray diffraction analysis, thermal analysis, SEM observation, and physical property analysis, and the data compared to those of native chitosan fibers.

2. Experimental

2.1. Materials

Chitosan powder was purchased from Tea-hoon bio. Co., Ltd. Its degree of deacetylation (DD) was 92%, as determined by elemental analysis. Acetic anhydride and butyric anhydride were purchased from Junsei Chemical Co., and propionic anhydride and hexanoic anhydride came from Acros Chemical Co. All other chemicals were of reagent grade and were used without further purification.

2.2. Wet-spinning of chitosan

Chitosan fibers were prepared using the wet spinning method. A dope was prepared by dissolving 4% by weight of chitosan in a solution of 2% by volume aqueous acetic acid at room temperature. The dope was pre-filtered using a filter-press and placed in a hopper. By applying air pressure at 2 kgf/cm^2, the dope was passed from a stainless-steel spinneret to coagulation bath. After exiting the coagulation bath, the fibers were washed with hot and cold water by turns. A diagram of wet spinning apparatus is found in Fig. 1.

2.3. N-Acylation of chitosan fibers

A portion (7 g) of the chitosan fibers was suspended in 150 ml of methanol, and each (5 mol/GlcN) of acetic, propionic, butyric, hexanoic anhydrides was added. The mixture was stirred for a few minutes to remove air bubbles on the surface of these fibers and then shaken at 40 °C. After 24 h, the treated fibers were washed several times with 100% methanol, and air-dried. The degree of substitute for *N*-acyl group was obtained from the C/N ratio, as obtained by elemental analysis.

2.4. Measurements

FT-IR spectroscopy was used to characterize chemical functional groups of chitosan and *N*-acyl chitosan fibers. FT-IR spectra (AVATAR 370, Thermo Nicolet) were collected using a KBr method. Elemental analysis was used to determine the degree of substitution of the *N*-acyl groups on chitosan chains. The measurement was carried out on a Thermo-Finnigan Flash 112 series. The X-ray diffraction was used to observe the crystal structure of the chitosan and *N*-acyl chitosan fibers. The XRD patterns were recorded at room temperature using a X-ray diffractometer (XRD; PW 1700, Philips) with a CuKα radiation generated at 40 kV and 30 mA. The thermal properties were measured by differential scanning calorimetry(DSC; TA Instruments Q 100, Perkin-Elmer) at a heating rate of 10 °C/min under N_2 atmosphere and thermogravimetric analysis (TGA; TA Instruments Q 500, Perkin-Elmer) at a heating rate of

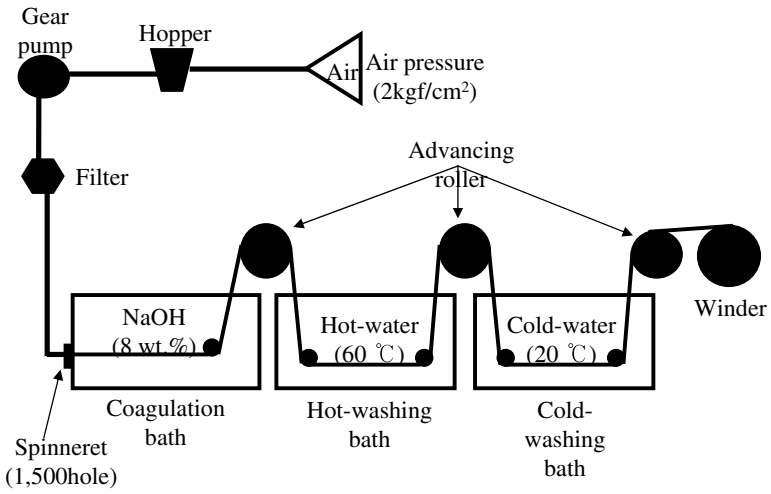

Fig. 1. Schematic diagram of wet-spinning apparatus.

10 °C/min under N_2 atmosphere from 30 to 600 °C. The tensile properties of the mono-fibers were measured with Tensilon (SEARCH Co.) at a crosshead speed of 20 mm/min. The surface morphologies of chitosan and *N*-acyl chitosan fibers were observed using a scanning electron microscope (SEM; JSM-6300, JEOL). SEM observations were conducted at an accelerating voltage of 15 kV and all samples were coated with gold before scanning.

3. Results and discussion

3.1. Characteristics of N-acyl chitosan fibers

The *N*-acyl chitosan fibers were prepared under homogeneous conditions using a series of carboxylic anhydrides of 5.0 mol per glucosamine residue (Fig. 2). The structure of *N*-acyl chitossan fibers was identified by FT-IR analysis. Fig. 3 shows the FT-IR spectra of chitosan and *N*-acyl chitosan fibers. There existed characteristic peaks of chitosan at 2940 ($-CH_3$, $-CH_2$), 1665 (C═O stretch vibration), 1560 (secondary amide), and 1070 cm^{-1}(C—O). In the case of *N*-acyl chitosan fibers, the peaks were gradually sharpened at 2880, 2940 cm^{-1} (C—H for hydro-carbon) and 1560, 1665 cm^{-1}(C═O and N—H for *N*-acyl) with an increasing acyl chain length, but no *O*-acyl absorption was detected at ~700 cm^{-1}. Also, the degree of substitution (d.s.) for *N*-acyl group was calculated from the C/N ratio of the elemental analysis. The results obtained suggested that the values of d.s. for *N*-acyl group were in the range of 0.64–0.84 (Table 1). Through the FT-IR analysis and the elemental analysis, we confirmed that the chitosan fibers were selectively *N*-acylated in the range of 0.64–0.84 after treatment with a series of carboxylic anhydrides in methanol.

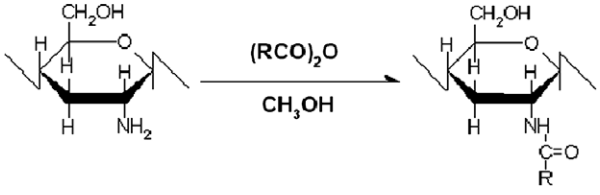

Fig. 2. Heterogeneous acylation reaction of chitosan with a series of carboxylic anhydrides in methanol.

3.2. X-ray diffraction

The X-ray diffraction patterns of chitosan fibers and *N*-acyl chitosan fibers with a series of carboxylic anhydrides treatments are shown Fig. 4. According to the structural analysis by X-ray diffraction, the crystalline structure was gradually altered by *N*-acylation of chitosan fibers. A XRD pattern of the chitosan shows a moderately sharp intense diffraction at the (040) plane near $2\theta = 20.2°$ and a less intense diffraction at the (020) plane near $2\theta = 10.2°$ (Lee, 2000). However, by the increasing acyl chain length by *N*-acylation of chitosan fibers, the X-ray diffractogram intensity near $2\theta = 10°$ were comparatively sharpened, respectively. The presence of this transition is considered as

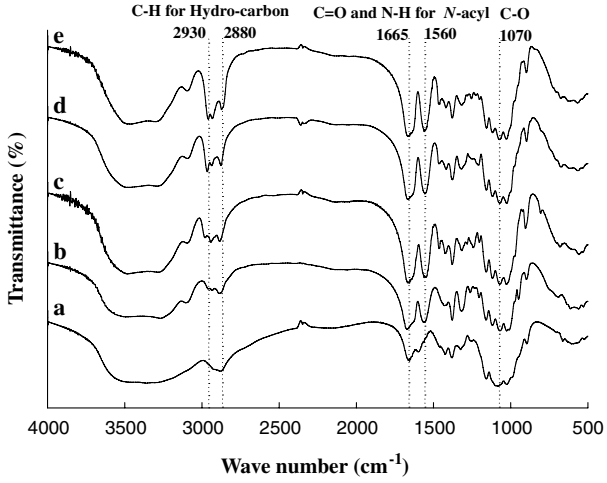

Fig. 3. FT-IR spectra of (a) Chitosan, (b) *N*-acetyl, (c) *N*-propionyl, (d) *N*-butyryl, (e) *N*-hexanoyl chitosan fibers.

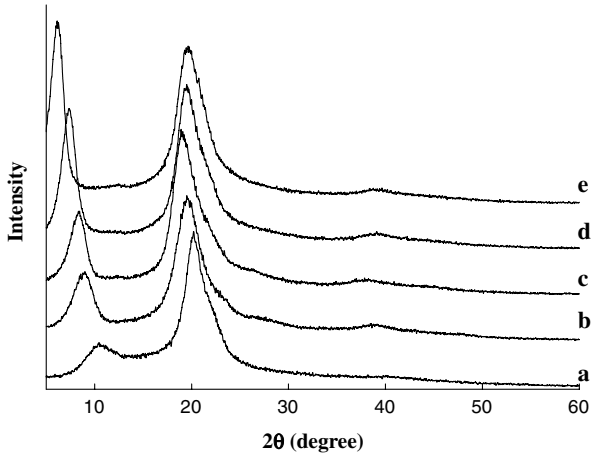

Fig. 4. The XRD patterns of (a) Chitosan, (b) *N*-acetyl, (c) *N*-propionyl, (d) *N*-butyryl, (e) *N*-hexanoyl chitosan fibers.

Table 1
Elemental analysis and d.s. for *N*-acyl chitosan and *N*-acyl chitosan fibers

N-Substituted group	Anal. Calc. (%)			Found (%)			d.s. for *N*-acyl
	C	H	N	C	H	N	
N-Acetyl	43.90	6.74	6.40	41.22	6.89	6.32	0.80
N-Propionyl	46.53	7.19	6.03	44.65	7.22	6.57	0.64
N-Butyryl	48.97	7.59	5.71	47.28	7.64	6.14	0.75
N-Hexanoyl	52.51	7.59	5.11	52.07	8.30	5.49	0.84

the level of long-range order required to increase the fibers axis. We conjectured that the large number of hydrogen bonding in the chitosan fibers was destroyed through the *N*-acylation, thus forming a better spatial organization of the chain to the long axis.

3.3. Thermal properties

To research the thermal properties of chitosan and *N*-acyl chitosan fibers, we performed TGA and DSC analysis. In general, the thermal properties of chitosan and chitosan derivatives are similar to those of cellulose. They do not melt but degrade at elevated temperatures. Fig. 5 presents the results of TGA curves of chitosan fibers and *N*-acyl chitosan fibers. The chitosan fiber was thermally decomposed in the region of 280–320 °C, whereas the thermal decomposition of *N*-acyl chitosan fibers was occurred in the region of 320–400 °C. Thus, we believed that the *N*-acylation provides the chitosan fibers with thermal stability. According to the region denoted by "(A)", the longer the acyl chain length of chitosan fibers, the lower water content. We believed that *N*-acylation of chitosan fibers lead to the dehydration of the fibers.

Fig. 6 presented that the DSC thermograms of chitosan and *N*-acyl chitosan fibers. In the case of chitosan fibers, a strong exothermal peak occurred within the temperature interval of 280–320 °C. Conversely, *N*-acyl chitosan fibers showed an endothermal depression within the temperature interval 320–390 °C and a stronger depression for longer acyl chains. This results suggested that the exothermal peak of chitosan fibers occurred by an exothermal reaction within the polymer and the endothermal depression of *N*-acylchitosan fibers seemed to be a thermal decomposition of the crystalline regions. Also, this behavior suggested a higher crystallinity for a longer acyl chain.

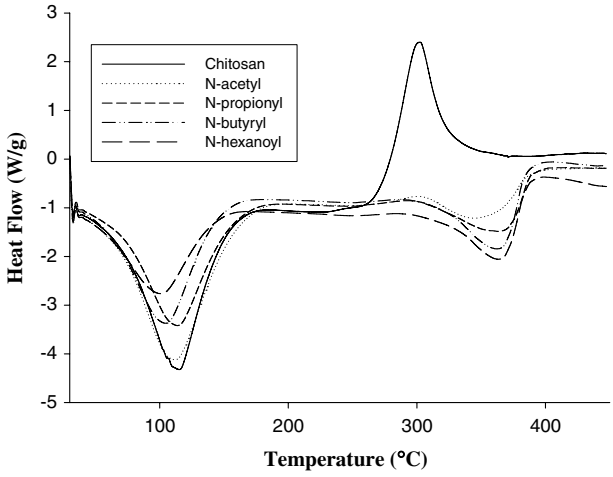

Fig. 6. DSC thermograms of chitosan and *N*-acyl chitosan fibers.

3.4. Mechanical properties

The tensile testing results of chitosan and *N*-acyl chitosan fibers are presented in Fig. 7. The *N*-acyl chitosan fibers with short acyl chain exhibited gradually weaker tensile strength and higher elongation than chitosan fibers, probably due to hydrogen bonding destruction by *N*-acylation. But, in case of *N*-hexanoyl chitosan fibers, which has longer acyl chain, the tensile strength was higher than *N*-aceyl chitosan fibers. The explanation for this behavior may reside in the intensity of hydrophobic interactions, which for longer acyl chain and a higher degree of substitution can stabilize the structure (Le Tien, Lacroix, Ispas-Szabo, & Mateescu, 2003). In this study, if we prepare *N*-acylation of chitosan fibers with longer hydro-carbon side chain than *N*-hexanoyl chitosan fibers, its respective tensile strength would higher than *N*-hexanoyl chitosan fibers.

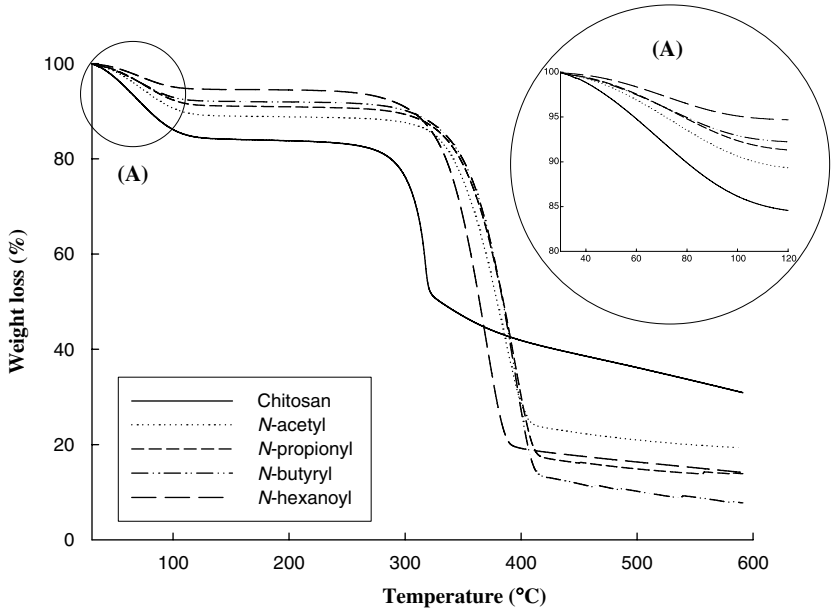

Fig. 5. TGA curves of chitosan and *N*-acyl chitosan fibers.

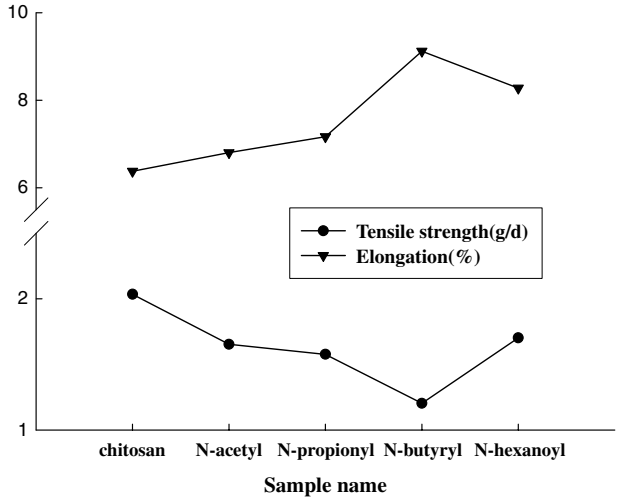

Fig. 7. Tensile strength and elongation of chitosan and *N*-acyl chitosan fibers.

3.5. Surface morphology

Fig. 8 shows SEM photographs of chitosan fibers and *N*-hexanoyl chitosan fibers. The surface pattern of chitosan fibers was very smooth, whereas *N*-hexanoyl chitosan fibers showed a slightly rougher and stretched surface pattern. Essentially the same surface patterns were observed with the other *N*-acyl chitosan fibers. The slightly rough and stretched pattern is considered to be formed by dehydration and a neutralization processes during *N*-acylation of chitosan fibers.

3.6. Chemical structure transition by N-acylation of chitosan fibers

Demarger-Andre and Domard reported that anhydrous chitosan crystals can be obtained at room temperature from chitosan salts of several monocarboxylic acids by spontaneous removal of the acids accompanied by dehydrations (Demarger-Andre & Domard, 1994). Also, C. Le Tien et al. reported that the longer side chain and higher degree of substitution on the *N*-acyl chitosan were able to enhance the stability of substituted chitosan via "hydrophobic self-assembly" (Le Tien et al., 2003). Through the previous paper and the results of physico-chemical properties in this study, we were able to confirm that the chemical structure of chitosan fibers was altered newly by the introducing of *N*-acyl group. This chemical structure transition of chitosan fibers by the *N*-acylation may be explained by Fig. 9. Untreated chitosan(hydrated chitosan) fibers are randomly stabilized by intramolecular O(3′)H…O(5), intermolecular NH…O(6) hydrogen bonding and hydrogen bridging involving water molecules. Through the introducing *N*-acyl group to amine group of chitosan fibers by *N*-acylation, the breakage of the hydrogen bonds and the dehydration were immediately occurred. Therefore the entire crystalline structure of chitosan was destabilized by increasing the main chain mobility. Sequentially the activated main chain tended to move toward a kinetically ideal form. As a result of this tendency, parallel main chains were organized in sheet structures via new intermolecular interaction, and at this time the length of substituted hydro-carbon chain resulted in the destruction and new formation of hydrogen bonding C(2)NH…O(6) so that the general properties (crystalline, physical and thermal. etc.) were reflected. In the case of short hydro-carbon chain introduction or lower degree of substitution form, the physical property was poor in spite of an improvement in the crystalline structure because only a few hydrogen bonds were constituted. Meanwhile the hydrophobic interactions enhance the stability and participate in a self-assembled network organization according to the longer hydro-carbon chain introduction or higher degree of substitution form.

4. Conclusion

N-Acyl chitosan fibers (*N*-acetyl, *N*-propionyl, *N*-btyryl, *N*-hexanoyl) were prepared with a various carboxylic anhydrides in methanol at room temperature. Chitosan fibers were selectively *N*-acylated in the d.s. range of 0.64–0.84. With the increase of acyl chains length, the main chain structure contained more crystalline regions and the capacity to hydrate was gradually lost. *N*-Acylation lowered the tensile

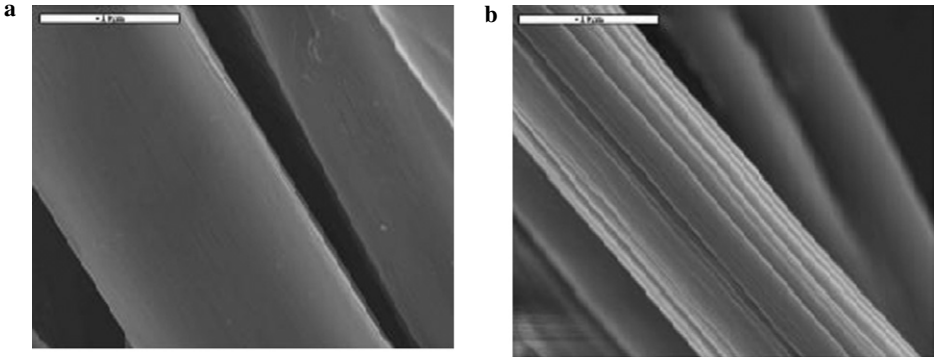

Fig. 8. SEM photographs of chitosan fiber (a) and *N*-hexanoyl chitosan fiber (b).

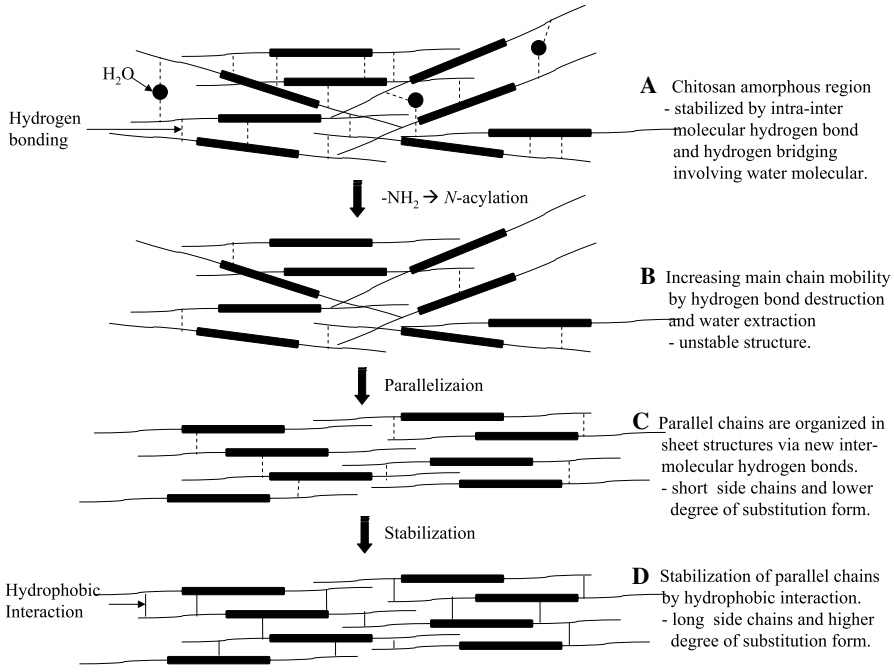

Fig. 9. The schematic presentation of chemical structure transition by *N*-acylation of chitosan fiber.

strength of chitosan fibers by hydrogen bonding breakage. However, despite of longer hydrocarbon chain, *N*-hexanoyl chitosan fibers showed the slightly improved strength due to the hydrophobic interaction. From this study, we are confirmed that the hydrated form (antiparallel) chitosan fibers which have inter-intra molecular hydrogen bonding and hydrogen bridging involving water molecules was converted to a dehydrated form with the molecular packing and water content quite different by *N*-acylation. It suggested that the crystallinity, physico-chemical stability and hydrophobicity of the chitosan fibers could be controlled by *N*-acylation depending on both the acyl chain length and the degree of acylation.

Acknowledgments

This work was supported by Grant No. RTI04-01-04 from the Regional Technology Innovation Program of the Ministry of Commerce, Industry, and Energy (MOCIE).

References

Clark, G., & Smith, A. F. (1937). X-ray diffraction of chitin, chitosan, and derivatives. *Journal of Physical Chemistry, 40*(7), 863–879.

Demarger-Andre, S., & Domard, A. (1994). Chitosan carboxylic acid salts in solution and in the solid state. *Carbohydrate Polymers, 23*, 211–219.

George, C. E., & Yimin, Q. (1993). Wet spinning of chitosan and the acetylation of chitosan fibers. *Journal of Applied Polymer Science, 50*, 1773–1779.

Hirano, S., & Midorikawa, T. (1998). A novel method for the preparation of *N*-acylchitosan fibre and *N*-acylchito-san-cellulose fibre. *Biomaterials, 19*, 293–297.

Hirano, S., & Noishiki, Y. (1985). The blood compatibility of chitosan and *N*-acylchitosans. *Journal of Biomedical Materials Research, 19*, 413–417.

Hirano, S., Ohe, Y., & Ono, H. (1976). Selective *N*-acylation of chitosan. *Carbohydrate Research, 47*, 315–320.

Hirano, S., Zhang, M., Chung, B. G., & Kim, S. K. (2000). The *N*-acylation of chitosan fibre and the *N*-deacetylation of chitin fibre and chitin–cellulose blended fibre at a solid state. *Carbohydrate Polymers, 41*, 175–179.

Kawada, J., Abe, Y., Yui, T., Okuyama, K., & Ogawa, K. (1999). Crystalline transformation of chitosan from hydrated to anhydrous polymorph via chitosan monocarboxylic acid salts. *Journal of carbohydrate chemistry, 18*, 559–571.

Lee, S. H. (2000). The mechanism and characteristics of dry-jet wet spinning of chitosan fibers. *The Journal of Korean Fiber Society, 37*, 374–381.

Le Tien, C., Lacroix, M., Ispas-Szabo, P., & Mateescu, M. A. (2003). *N*-Acylated chitosan: hydrophobic matrices for controlled drug release. *Journal of Controlled Release, 93*, 1–13.

Majuti, N. V., & Kumar, R. (2000). A review of chitin and chitosan applications. *Reactive and Functional Polymers, 46*, 1–27.

Mohamed, N. S., Subban, R. H. Y., & Arof, A. K. (1995). Polymer batteries fabricated from lithium complexed acetylated chitosan. *Journal of Power Sources, 56*, 153–156.

Mori, T., Okamura, M., Matsuura, H., Ueno, K., Tokura, S., Okamoto, Y., et al. (1997). Effects of chitin and its derivatives on the proliferation and cytokine production of fibroblasts in vitro. *Biomaterials, 18*, 947–951.

Okuyame, K., Noguchi, K., Kanenari, M., Egawa, T., Osawa, K., & Ogawa, K. (2000). Structural diversity of chitosan and its complexes. *Carbohydrate Polymers, 41*, 237–247.

Okuyama, K., Noguchi, K., Miyazawa, T., Yui, T., & Ogawa, K. (1997). Molecular and crystal structure of hydrated chitosan. *Macromolecules, 30*, 5849–5855.

Rudall, K. M. (1963). The chitin/protein complexes of insect cuticles. *Advances in Insect Physiology, 1*, 257–313.

Samuels, R. J. (1981). Solid state characterization of the structure of chitosan films. *Journal of Polymer Sciences, 19*, 1081–1105.

Shigemasa, Y., & Minami, S. (1995). Applications of chitin and chitosan for biomaterials. *Biotechnology and Gene Engineering Review, 13*, 383–420.

Tokura, S., Baba, S., Uraki, Y., Miura, Y., Nishi, N., & Hasekawa, O. (1990). Carboxymethyl-chitin as a drug carrier of sustained release. *Carbohydrate Polymers, 13*, 273–281.

Yui, T., Imada, K., Okuyama, K., Obata, Y., Suzuki, K., & Ogawa, K. (1994). Molecular and crystal structure of the anhydrous form of chitosan. *Macromolecules, 27*, 7601–7605.